

Holographic entanglement entropy in nonlocal theories

Joanna L. Karczmarek and Charles Rabideau

*Department of Physics and Astronomy
University of British Columbia, Vancouver, Canada*

Abstract

We compute holographic entanglement entropy in two strongly coupled nonlocal field theories: the dipole and the noncommutative deformations of SYM theory. We find that entanglement entropy in the dipole theory follows a volume law for regions smaller than the length scale of nonlocality and has a smooth cross-over to an area law for larger regions. In contrast, in the noncommutative theory the entanglement entropy follows a volume law for up to a critical length scale at which a phase transition to an area law occurs. The critical length scale increases as the UV cutoff is raised, which is indicative of UV/IR mixing and implies that entanglement entropy in the noncommutative theory follows a volume law for arbitrary large regions when the size of the region is fixed as the UV cutoff is removed to infinity. Comparison of behaviour between these two theories allows us to explain the origin of the volume law. Since our holographic duals are not asymptotically AdS, minimal area surfaces used to compute holographic entanglement entropy have novel behaviours near the boundary of the dual spacetime. We discuss implications of our results on the scrambling (thermalization) behaviour of these nonlocal field theories.

Contents

1	Introduction	1
2	Theories considered and their gravity duals	4
2.1	NCSYM	4
2.2	Dipole theory	6
3	Entanglement entropy for the strip	8
3.1	Review of results for AdS space	9
3.2	Dipole theory	10
3.3	NCSYM	13
4	Entanglement entropy for the cylinder in NCSYM	17
5	Mutual information in NCSYM	21
6	Final comments	22

1 Introduction

Geometric entanglement entropy as a tool to characterize physical properties of quantum field theories has recently received a large amount of attention. One attractive feature of geometric entanglement entropy as an observable is that it is defined in the same way in any quantum field theory: it is simply the von Neumann entropy, $-\text{Tr}(\rho_A \log \rho_A)$, associated with the density matrix ρ_A describing degrees of freedom living inside a region A . ρ_A arises when the portion of total Hilbert space associated with degrees of freedom living outside of A is traced over. Universality of entanglement entropy is reflected in the Ryu-Takayanagi holographic formula [1]

$$S[A] = \frac{\text{Vol}_d(\tilde{A})}{4G_N^{(d+2)}} . \tag{1}$$

Here, we place A , a d -dimensional spacial region, on a spacelike slice of the boundary of the $(d+2)$ -dimensional spacetime dual to the quantum field theory of interest. \tilde{A} is a minimal area surface in the bulk of the holographic dual spacetime homologous to A . $G_N^{(d+2)}$ is the $(d+2)$ -dimensional Newton constant and the d -dimensional volume of \tilde{A} is denoted with $\text{Vol}_d(\tilde{A})$.¹

The Ryu-Takayanagi formula (1) is applicable to holographic duals where the dilaton and the volume of the internal sphere are both constant. However, duals to the nonlocal theories

¹For an accessible introduction and some recent developments to holographic entropy, see for example [2, 3].

we are interested in have neither, so the local gravitational constant $G_N^{(d+2)}$ varies. Thus we must use a generalized version of formula (1), given by [4]

$$S[A] = \frac{\text{Vol}(\bar{A})}{4G_N^{(10)}}, \quad \text{with } \text{Vol}(\bar{A}) = \int d^8\sigma e^{-2\phi} \sqrt{G_{\text{ind}}^{(8)}}, \quad (2)$$

where $G_N^{(10)} = 8\pi^6(\alpha')^4 g_s^2$ is the (asymptotic) 10-dimensional Newton's constant and ϕ is the local value of the fluctuation in dilaton field (so that the local value of the 10-dimensional Newton's constant is $G_N^{(10)} e^{2\phi}$). Integration is now over a co-dimension two surface \bar{A} that wraps the compact internal manifold of the holographic dual.

Because \bar{A} wraps the internal manifold, its boundary is the direct product of the boundary of A , ∂A , and the internal manifold. To obtain entanglement entropy, \bar{A} is chosen to have minimal area (we will only work in static spacetimes). $G_{\text{ind}}^{(8)}$ is the induced string frame metric on \bar{A} . By considering the standard relationship between local Newton's constants in different dimensions: $G_N^{(d+2),\text{local}} = G_N^{(10)} e^{2\phi} / V_{8-d}$, together with $\text{Vol}(\bar{A}) = V_{8-d} \text{Vol}_d \tilde{A}$, equation (1) can be easily recovered from (2) for a scenario where the dilaton is a constant and the internal manifold has a constant volume V_{8-d} (in string metric). The more general formula (2) has been used to study, for example, tachyon condensation [5] and confinement-deconfinement transition [6]. We will refer to the 8-dimensional $\text{Vol}(\bar{A})$ as the area of the minimal surface from now on.

Generically, geometric entanglement entropy has a UV divergence, so it needs to be regulated with a UV cutoff. Holographically, this is accomplished the usual way by placing the region A on a surface which is removed from the boundary of the holographic dual spacetime. Once the theory has been regulated with a cutoff, geometric entanglement entropy in the vacuum state can be thought to count effective degrees of freedom inside A that have quantum correlations with degrees of freedom outside of A . In other words, it measures the range of quantum correlations generated in the ground state by the interactions in the Hamiltonian. For a local theory, degrees of freedom with correlations across the boundary of A must live near this boundary, which leads to the area law: entanglement entropy in local theories is generically proportional to the area of the boundary of A , $|\partial A|$. While the area law has not been proven for a general interacting field theory, it is expected to generically hold in local theories for the reason outlined above (see [7] for a review, focusing on lattice systems).

In a nonlocal theory, behaviour of entanglement entropy could be expected to deviate from the area law and this is precisely what we find using holographic methods at strong coupling. In a simple nonlocal theory with a fixed scale of nonlocality a_L , a dipole deformation of $\mathcal{N} = 4$ SYM, we find that entanglement entropy is extensive (proportional to the volume of A), for regions A of size up to a_L . At length scales higher than a_L , it follows an area law, with an effective number of entangled degrees of freedom which is proportional to a_L . This is consistent with all degrees of freedom within a region A of size a_L or smaller, and not

only those living close to the boundary of A , having quantum correlations with the outside of A due to the nonlocal nature of the Hamiltonian. In contrast, in the noncommutative deformation of $\mathcal{N} = 4$ SYM, which is known to exhibit UV/IR mixing and whose nonlocality length scale grows with the UV cutoff, we find that entanglement entropy is extensive for all regions as long as their size is fixed as the UV cutoff is taken away to infinity.²

Recent work [9] links behaviour of entanglement entropy to the ability of a quantum system to ‘scramble’ information. Whether a given physical theory is capable of scrambling, and how fast it can scramble, has recently become of interest to the gravity community in the view of the so called fast scrambling conjecture [10]. It has been suggested that nonlocal theories might emulate the scrambling behaviour of stretched black hole horizons. While the results of [9] do not apply directly to quantum field theories, they are quite suggestive. Generally speaking, they imply that local (lattice) theories, generally exhibiting area law for entanglement entropy at low energies, do not scramble information at these low energies, while theories with volume law entanglement entropy do. As we summarized above, we demonstrate here, in the two nonlocal theories we consider, that entanglement entropy follows a volume law in the vacuum state. There is no reason why entanglement entropy would cease to be extensive in an excited energy state; if anything, high energy states are more likely to have extensive entanglement entropy than low-lying states such as the vacuum state [11, 12]. Thus, the results of [9] would suggest that our nonlocal theories are capable of scrambling information. Combined with such results as those in [13], which shows that timescales for thermalization in nonlocal theories are accelerated compared to local theories, our work points towards these nonlocal theories at strong coupling being fast scramblers.

Since our theories differ from $\mathcal{N} = 4$ SYM in the UV, holographic duals to we use are not asymptotically AdS spaces. Their non-asymptotically AdS geometry has an interesting consequence. In previously studied examples of extensive behaviour of entanglement entropy (for example, in thermal states) this extensive behaviour was due to the minimal surface ‘wrapping’ a surface in the IR region of the dual, such as a black hole horizon (see for example [14]). Here, however, the extensivity arises from the fact that the minimal surfaces stays close to the cutoff surface: the volume law dependence of entanglement entropy is a UV phenomenon.

As we were finalizing this manuscript, preprint [15] appeared, which also analyzes entanglement entropy in the noncommutative SYM and which has some overlap with our work.

The remainder of the paper is organized as follows: in Section 2 we review nonlocal theories of interest and their gravity duals, in Section 3 we compute holographic entanglement entropy for a strip geometry, in Section 4 we compute holographic entanglement entropy in the noncommutative theory for a cylinder geometry, in Section 5 we briefly comment on mutual information in the noncommutative theory, and in Section 6 we offer further discussion of

²Entanglement entropy in the noncommutative theory was studied before in [8]. Here we extend and improve on those results.

our results.

2 Theories considered and their gravity duals

We study the strong coupling limit of two different nonlocal deformations of $\mathcal{N}=4$ SYM in 3+1 dimensions: a noncommutative deformation and a dipole deformation. Both of these can be realized as the effective low energy theory on D3-branes with a background NSNS B-field. To obtain the non-commutative deformation, both indices of the B-field must be in the worldvolume of the D3-brane, while to obtain the dipole theory, one of the indices must be in the worldvolume of the D3-brane while the other one must be in an orthogonal (spacial) direction.

Since both of these theories are UV deformations of the $\mathcal{N}=4$ SYM, deep in the bulk their holographic duals reduce to pure AdS:

$$\frac{ds^2}{R^2} = u^2 (-dt^2 + dx^2 + dy^2 + dz^2) + \frac{du^2}{u^2} + d\Omega_5^2 \quad (3)$$

with a constant dilaton:

$$e^{2\phi} = g_s^2 . \quad (4)$$

In our coordinates, the boundary of AdS space, corresponding to UV of the field theory, is at large u . It is in that region that the holographic duals in the next two sections will deviate from the above.

2.1 NCSYM

Noncommutative Yang-Mills theory is a generalization of ordinary Yang-Mills theory to a noncommutative spacetime, obtained by replacing the coordinates with a noncommutative algebra. We consider a simple set up where the x and y coordinates are replaced by the Heisenberg algebra, for which $[x, y] = i\theta$ and which corresponds to a noncommutative $x - y$ plane.

One way to define this noncommutative deformation of $\mathcal{N}=4$ SYM is to replace all multiplication in the Lagrangian with a noncommutative star product:

$$(f \star g)(x, y) = e^{\frac{i}{2}\theta\left(\frac{\partial}{\partial\xi_1}\frac{\partial}{\partial\zeta_2} - \frac{\partial}{\partial\zeta_1}\frac{\partial}{\partial\xi_2}\right)} f(x + \xi_1, y + \zeta_1)g(x + \xi_2, y + \zeta_2) \Big|_{\xi_1=\zeta_1=\xi_2=\zeta_2=0} \quad (5)$$

At low energy, this corresponds to deforming ordinary SYM theory by a gauge invariant operator of dimension six.

The holographic dual to this noncommutative SYM theory is given by the following bulk data [16, 17]

$$\frac{ds^2}{R^2} = u^2 (-dt^2 + f(u) (dx^2 + dy^2) + dz^2) + \frac{du^2}{u^2} + d\Omega_5^2 ,$$

$$\begin{aligned}
e^{2\phi} &= g_s^2 f(u) , \\
B_{xy} &= -\frac{1-f(u)}{\theta} = -\frac{R^2}{\alpha'} a_\theta^2 u^4 f(u) , \\
f(u) &= \frac{1}{1+(a_\theta u)^4} ,
\end{aligned} \tag{6}$$

where B_{xy} is the only nonzero component of the NS-NS form background. Note that x, y, z have units of length, while u has units of length inverse, or energy. $a_\theta = (\lambda)^{1/4} \sqrt{\theta}$ is the weak coupling length scale of noncommutativity $\sqrt{\theta}$ scaled by a power of the 't Hooft coupling λ and can be thought of as the length scale of noncommutativity at strong coupling.

In the infrared limit, $u \ll a_\theta^{-1}$, $f(u) \approx 1$ and the holographic dual appears to approach pure AdS space (3), while the UV region at large u is strongly deformed from pure AdS, so the holographic dual is not asymptotically AdS. Let ϵ denote the UV cutoff and $u_\epsilon = \epsilon^{-1}$ the corresponding energy cutoff. For $\epsilon \gg a_\theta^{-1}$ ($u_\epsilon \ll a_\theta^{-1}$), the deformed UV region of the dual spacetime is removed: noncommutativity has been renormalized away. However, when $u_\epsilon > a_\theta^{-1}$, the non-AdS geometry near the boundary can influence the holographic computations of any field theory quantities, including those with large length scales. This opens the possibility of UV/IR mixing, defined as sensitivity of IR quantities to the exact value of the UV cutoff. Noncommutative theories are known to have UV/IR mixing [18]. The simplest way to understand the mechanism behind the UV/IR mixing in noncommutative theories is to consider fields with momentum p_y in the y -direction in equation (5): $f(x, y) = e^{-ip_y^f y} \hat{f}(x)$, $g(x, y) = e^{-ip_y^g y} \hat{g}(x)$. Then $f \star g(x, y) = e^{-i(p_y^g + p_y^f)y} \hat{f}(x - \theta p_y^g/2) \hat{g}(x + \theta p_y^f/2)$: the interaction in the x -direction is nonlocal on a length scale θp_y . We will see that this momentum (or energy) dependence of the scale of nonlocality is reflected in holographic entanglement entropy.

Finally, we need to understand the geometry of the boundary. The metric on the boundary of the gravitational spacetime (6) is singular since $f \rightarrow 0$ there. However, this is not the metric applicable to the boundary field theory, as open string degrees of freedom see the so-called open string metric. This is the effective metric which enters open-string correlation functions in the presence of a NS-NS potential B , first derived in [19]³ and given by

$$G_{ij} = g_{ij} - (Bg^{-1}B)_{ij} , \tag{7}$$

where g_{ij} is the closed string metric. Substituting our holographic data at a fixed u , we obtain the open string metric, $G_{ij} = R^2 u^2 (\delta_{ij})$. Removing an AdS conformal factor, we see that the boundary field theory lives on a space with a conformally invariant metric $ds^2 = -dt^2 + dx^2 + dy^2 + dz^2$. This is the metric we will use to compute distances on the field theory side of the holographic correspondence.

³For an interpretation of the open string metric in the context of the AdS-CFT duality, see for example [20].

2.2 Dipole theory

Another theory we will consider is the simplest dipole deformation of $\mathcal{N} = 4$ SYM [21, 22, 23]. A dipole theory is one in which multiplication has been replaced by the following non-commutative product:

$$(f\tilde{\star}g)(\vec{x}) = f\left(\vec{x} - \frac{\vec{L}_f}{2}\right)g\left(\vec{x} + \frac{\vec{L}_g}{2}\right), \quad (8)$$

where \vec{L}_f and \vec{L}_g are the dipole vectors assigned to fields f and g respectively. At low energy, this corresponds to a deformation by a vector operator of dimension 5. To retain associativity of the new product, we must assign a dipole vector $\vec{L}_f + \vec{L}_g$ to $f\tilde{\star}g$. A simple way to achieve it is to associate with each field f a globally conserved charge Q_f and to let $\vec{L}_f = \vec{L}Q_f$. This can also be easily extended to multiple globally conserved charges. We will take $\vec{L} = L\hat{x}$ for some fixed length scale L , so that our theory is nonlocal only in the x -direction. As we saw in the previous section, noncommutative theory can be thought of as a dipole theory with the charges being momenta in a direction transverse to the dipole direction.⁴

Dipole SYM is a simpler nonlocal theory than the NCSYM. Since the scale of the noncommutativity is fixed, the theory does not exhibit UV/IR mixing. We will see a clear signature of that in the entanglement entropy.

The holographic dual to a dipole deformation of $\mathcal{N} = 4$ SYM theory where the scalar and fermion fields in $\mathcal{N} = 4$ SYM are assigned dipole lengths based on global R-symmetry charges was found, using Melvin twists, in [24]. For the simplest case, where supersymmetry is broken completely and where all the scalar fields have the same dipole lengths, the holographic dual is given by the following bulk data:

$$\begin{aligned} \frac{ds^2}{R^2} &= u^2(-dt^2 + f(u)(dx^2) + dy^2 + dz^2) + \frac{du^2}{u^2} + \text{metric on a deformed } S^5, \\ e^{2\phi} &= g_s^2 f(u), \\ B_{x\psi} &= -\frac{1-f(u)}{\tilde{L}} = -\frac{R^2}{\alpha'} a_L u^2 f(u), \\ f(u) &= \frac{1}{1+(a_L u)^2}. \end{aligned} \quad (9)$$

Similar to a_θ , $a_L = \lambda^{1/2}\tilde{L}$, $\tilde{L} = L/(2\pi)$ is the length scale of nonlocality at strong coupling. The usual S^5 of the gravity dual to a 3+1-dimensional theory is deformed in the following way: Express S^5 as S^1 fibration over $\mathbb{C}\mathbb{P}^2$ (the Hopf fibration). Then the radius of the fiber acquires a u -dependent factor and is given by $Rf(u)$. The volume of the $\mathbb{C}\mathbb{P}^2$ is constant

⁴This is not entirely accurate, as a field with transverse momentum p induces a dipole moment θp in all the fields it interacts with instead of in itself, but this detail will not be relevant to our reasoning.

and given by $R^4\pi^2/2$. Thus the compact manifold at radial position u has a volume given by $R^5\pi^3 f(u)$. ψ is the global angular 1-form of the Hopf fibration. For details, see [24].

As we did for the noncommutative theory in the previous section, we need to understand what metric to use for distances in the boundary dipole theory. Unfortunately, it does not seem possible to give an argument similar to the one in [19] to find an ‘open string metric’ for the D-branes whose low-energy theory gives us the dipole theory, since (in contrast to the noncommutative case) the dipole theory requires a nonzero NSNS field H and not just the nonzero potential B .⁵ The essence of the argument in [19] is that the only effect of the potential B is to change the boundary conditions for open string worldsheet theory. Thus, the boundary-boundary correlator is modified in a simple way that is equivalent to modifying the metric. To understand the open string metric for the dipole set up we need a different way to make the NSNS field B ‘disappear’. We can accomplish this following [24] and using T-duality.

First, let’s see what happens when we compactify the y direction in (6) on a circle of radius R_x and T-dualize using the prescription in [25]. The T-dual metric is

$$(Ru)^2 \left(-dt^2 + (dy - (\theta/\alpha')d\tilde{x})^2 + dz^2 \right) + \frac{1}{(Ru)^2}(d\tilde{x})^2 + \frac{du^2}{u^2} + d\Omega_5^2, \quad (10)$$

where \tilde{x} is the T-dual coordinate to x . In the T-dual, B is zero. It has been traded for the twist around the \tilde{x} circle: we identify (\tilde{x}, y) with $(\tilde{x} + 2\pi\tilde{R}_x, y + 2\pi\tilde{R}_x\theta)$, $R_x\tilde{R}_x \sim \alpha'$. Conformal invariance in the $t - y - z$ directions has been restored by T-duality, and we recover the open string metric (7) in those directions.⁶ At the same time, the twist encodes the nonlocal structure of the theory. To see this recall that in the noncommutative theory, fields with momentum p_x in the x -direction appear to have dipole lengths θp_x . Taking x on a circle of radius R_x , $p = n/R_x$, with n an integer. When T-dualized, the corresponding open string mode has winding number n in the \tilde{x} direction. Given the twist, the ends of this open string are separated by $\Delta y = 2\pi\tilde{R}_x(\theta/\alpha')n$. Substituting $n = R_x p$ we get $\Delta y \sim \theta p$: the twist reproduces nonlocal behaviour of the noncommutative theory when the distances are measured in the conformally invariant (or open string) metric.

Returning to the dipole theory, we perform T-duality in the direction of the Hopf fiber to obtain

$$(Ru)^2 \left(-dt^2 + (dx - \tilde{L}d\tilde{\psi})^2 + dy^2 + dz^2 \right) + \frac{(\alpha')^2}{R^2}(d\tilde{\psi})^2 + \frac{du^2}{u^2} + d(\mathbb{CP}^2). \quad (11)$$

Again, the NSNS potential $B_{\psi x}$ has been replaced by a twist. However, due to the twist of the Hopf fibration, in the T-dual there is a new NSNS potential component, B_{xb} where

⁵A constant potential B which has only one of its indices in the worldvolume of a D-brane can be gauged away completely. It is therefore important that the other index is in a direction of a circle with varying radius, resulting in a nonzero H . In the holographic dual we consider, this circle is the Hopf fiber.

⁶This is not a coincidence; the equation for the T-dual metric [25] and the equation for the open string metric (7) are functionally the same.

b lies in the direction of the \mathbb{CP}^2 , resulting in a nontrivial NSNS field H_{xbu} . Since ψ was a Dirichlet direction before T-duality, the interpretation is slightly different than it was in the noncommutative case. After T-duality, we have a twisted compactification identifying $(\tilde{\psi}, x)$ with $(\tilde{\psi} + 2\pi, x + 2\pi\tilde{L})$. The proper distance between $(\tilde{\psi}, x)$ and $(\tilde{\psi}, x + 2\pi\tilde{L})$ is therefore α'/R , which is small on the boundary in the large u limit. This is a sign of the nonlocality at the dipole length $L = 2\pi\tilde{L}$. More relevant to us at this point is that, just like for the noncommutative theory, conformal invariance in the $t - x - y - z$ direction has been restored in the T-dual metric. It seems reasonable then to use the metric $-dt^2 + dx^2 + dy^2 + dz^2$ to compute distances on in the boundary theory. For more details about this argument, as well as a string worldsheet argument about the origin of dipole theories, see [24, 26].

3 Entanglement entropy for the strip

We will start by studying entanglement entropy for degrees of freedom living on an infinitely long strip⁷ $-l/2 < x < l/2$, $-W/2 < y, z < W/2$, $W \rightarrow \infty$. In this geometry, entanglement entropy follows the area law if it is independent of the strip width l . As we discussed in the Introduction, the relevant minimal surface is eight-dimensional; it wraps the compact (possibly deformed) sphere of the gravity dual and is homologous to the strip on the boundary in the non-compact dimensions. Its area is given by

$$\text{Vol}(\bar{A}) = \pi^3 R^8 W^2 \int_{-l/2}^{l/2} dx (u(x))^3 \sqrt{1 + \frac{(u'(x))^2}{f(u)(u(x))^4}}, \quad (12)$$

where function $u(x)$ specifies the embedding of the bulk minimal area surface. The above formula for the area in terms of $u(x)$, with the appropriate form for $f(u)$, is applicable to all bulk metrics we are interested in: while the noncommutative theory dual has more directions warped by a factor $f(u)$ than the dipole one, in the dipole theory there is another factor of $f(u)$ accounting for the deformation of the sphere on which the entangling surface is wrapped.

Following previous work, we can think of the problem of finding $u(x)$ corresponding to a minimal area surface as a dynamics problem in one dimension: x plays the role of time, $u(x)$ is the position and $u'(x)$ the velocity. Since the Lagrangian

$$\mathcal{L}(u, u') = u^3 \sqrt{1 + \frac{(u')^2}{f(u)u^4}} \quad (13)$$

⁷ In dimensions three and higher it would be perhaps more accurate to call this region a ‘slab’ rather than a ‘strip’; nevertheless, we will use established terminology.

does not depend explicitly on the ‘time’ x , there is a conserved Hamiltonian,

$$H = u' \frac{\partial \mathcal{L}(u, u')}{\partial u'} - \mathcal{L}(u, u') = - \frac{u^3}{\sqrt{1 + \frac{(u')^2}{f(u)u^4}}} . \quad (14)$$

The Hamiltonian H is equal to $-u_*^3$, where u_* is the smallest value of $u(x)$ on the entangling surface. This point of deepest penetration of the minimal surface into the bulk occurs at $x = 0$ by symmetry. $u'(x)$ vanishes there.

To implement the UV cutoff, differential equation (14) is to be solved with a boundary condition

$$u(x = \pm l/2) = u_\epsilon = \frac{1}{\epsilon} . \quad (15)$$

For some functions $f(u)$, equation (14) can be integrated explicitly. The answer is a hypergeometric function for $f(u) = 1$ or $f(u) = 1/(a_\theta u)^4$, and an elementary function for $f(u) = 1/(a_L u)^2$. For $f(u) = 1/(1 + (a_L u)^2)$ or $f(u) = 1/(1 + (a_\theta u)^4)$, equation (14) can only be studied using series expansions in different limits.

To compute the area of the minimal surface, it is useful to solve equation (14) for $u'(x)$ as a function of u and substitute the result into equation (12). We obtain

$$\text{Vol}(\bar{A}) = 2\pi^3 R^8 W^2 \int_{u_*}^{u_\epsilon} \frac{du}{u'} \frac{u^6}{(-H)} = 2\pi^3 R^8 W^2 \int_{u_*}^{u_\epsilon} \frac{du u^4}{u_*^3} \sqrt{\frac{u_*^6}{f(u)(u^6 - u_*^6)}} . \quad (16)$$

To obtain the area of the minimal surface in terms of l from this equation, given u_ϵ , it is necessary to find the relationship between u_* and l .

3.1 Review of results for AdS space

For pure AdS, with $f(u) = 1$, we can remove the boundary of AdS all the way to infinity, $u_\epsilon \rightarrow \infty$. Then, by integrating (14), we obtain a simple relationship between u_* and the width of the strip l :

$$lu_* = \frac{\Gamma(2/3)\Gamma(5/6)}{\sqrt{\pi}} \approx 0.8624 . \quad (17)$$

This relationship has a nice interpretation: holographic entanglement entropy for a structure of size l is given by the minimal surface that probes AdS bulk from the UV cutoff down to energy scales of order l^{-1} . Modes with wavelength longer than l do not contribute to the entanglement entropy.

To compute the leading order (for $u_\epsilon \rightarrow \infty$) behaviour of the area of the minimal surface, we can use equation (16). Since u_* depends only on l and not on u_ϵ (i.e., it remains finite in the $u_\epsilon \rightarrow \infty$ limit), the leading contribution to the area comes from large values of u . We can thus approximate

$$\text{Vol}(\bar{A}) = 2\pi^3 R^8 W^2 \int^{u_\epsilon} duu = \pi^3 R^8 \frac{W^2}{\epsilon^2} . \quad (18)$$

A more precise result for the entanglement entropy density is obtained from a next-to-leading order computation. It gives a universal term which is finite and independent of the cutoff:

$$\frac{S}{W^2} = \frac{R^3}{4G_N^{(5)}} \left[\frac{1}{\epsilon^2} - \frac{(2\Gamma(\frac{2}{3})\Gamma(\frac{5}{6}))^3}{\pi^{3/2}} \frac{1}{l^2} + (\text{terms that vanish for } \epsilon \rightarrow 0) \right]. \quad (19)$$

In terms of field theory variables, we have

$$\frac{R^3}{4G_N^{(5)}} = \frac{N^2}{2\pi}, \quad (20)$$

so that the divergent part of the entanglement entropy is proportional to $N^2\epsilon^{-2}$, with a numerical coefficient which is specific to strongly coupled $\mathcal{N} = 4$ SYM. The entanglement entropy is therefore of this generic form (applicable to 3+1 dimensions):

$$S = N_{\text{eff}} \frac{|\partial A|}{\epsilon^2} = N_{\text{eff}} \frac{W^2}{\epsilon^2} \quad (21)$$

with the number of effective on-shell degrees of freedom N_{eff} proportional to N^2 .

Formula (21) supports the following simple picture of entanglement entropy in theory with a local UV fixed point: A quantum field theory in 3+1 dimensions with a UV cutoff ϵ^{-1} can be thought of as having on the order of one degree of freedom per cell of volume ϵ^3 . The divergent part of the geometric entanglement entropy computed the vacuum state of such a theory is a measure of the effective number of degrees of freedom inside of a region A that have quantum correlations with degrees of freedom outside of A . In a local theory, only ‘adjacent’ degrees of freedom are coupled via the Hamiltonian and the simple intuition is that therefore quantum correlations between degrees of freedom inside of A and outside of A happen only across the boundary ∂A . Thus, the dominant part of the entanglement entropy comes from degrees of freedom which live within a distance ϵ of the boundary of A , with entanglement entropy proportional to the volume of this ‘skin’ region, equal to $\epsilon|\partial A|$. Dividing this volume by the volume of one cell, ϵ^3 , gives equation (21).

3.2 Dipole theory

Having briefly reviewed holographic entanglement entropy on a strip in undeformed SYM, we will now study it in the dipole theory.

In Figure 1, we show the relationship between l and u_* for the dipole theory. We see that it approaches the AdS result (17) for large strip widths l and that it deviates significantly from it for strips whose width is on the order of and smaller than a_L . For narrow strips, the entangling surface does not penetrate the bulk very deeply into the IR region. To study these, we assume that $u_* \gg a_L^{-1}$ and write $f(u) \approx (a_L u)^{-2}$. Here we get a pleasant surprise:

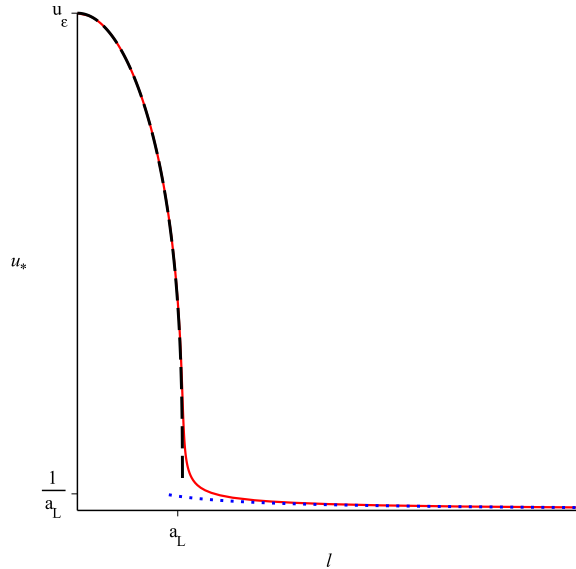


Figure 1: Point of deepest penetration u_* as a function of the strip width l for a minimal area surface in the gravity dual to the dipole theory (solid red line). The blue dotted line shows the result for pure AdS, given by equation (17), while the black dashed line shows the narrow strip approximation, equation (23). In this Figure, $a_L u_\epsilon = 30$.

the exact shape of the minimal surface can be obtained in terms of elementary functions

$$u(x) = \frac{u_*}{\cos(3x/a_L)^{1/3}} \quad \text{for } x/a_L \in [-\pi/6, \pi/6]. \quad (22)$$

The relationship between the penetration depth of the minimal surface and the width of the strip is

$$u_* = u_\epsilon (\cos(3l/2a_L))^{1/3}. \quad (23)$$

This equation is valid as long as $u_* \gg a_L^{-1}$, which, in the limit where u_ϵ is large, is true for all strip widths l up to $l = (\pi/3)a_L$. Notice that, in contrast to pure AdS, the point of deepest penetration u_* depends on the UV cutoff. Thus, if one works at the limit of infinite cutoff, these minimal area surfaces will be missed.

The area of the minimal surface under the approximation $f(u) \approx (a_L u)^{-2}$ is

$$\text{Vol}(\bar{A}) = \pi^3 R^8 \left[\frac{W^2 a_L}{\epsilon^3} \frac{2 \sin(3l/2a_L)}{3} \right] \approx \pi^3 R^8 \frac{W^2 l}{\epsilon^3}, \quad (24)$$

where the final approximation is for a small strip width $l \ll a_L$. For narrow strips, entanglement entropy is extensive, proportional to the width of the strip. The first part of equation (24) gives the corrections to the volume scaling, controlled by the powers of the ratio l/a_L .

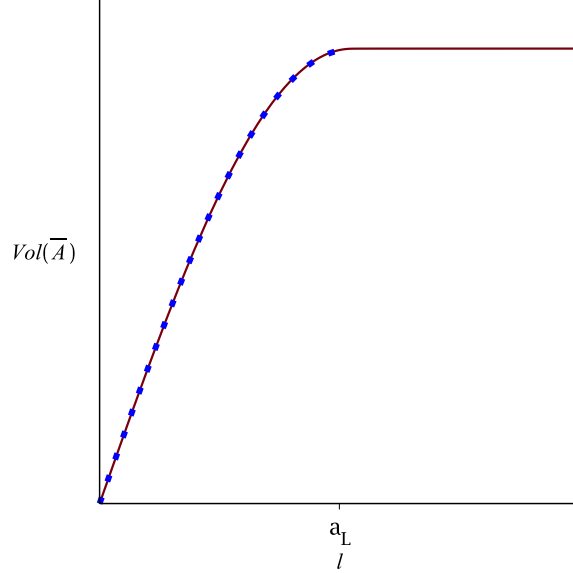


Figure 2: The area of the minimal surface as a function of the strip width l for for the dipole theory (solid red line). The blue dotted line shows result (24), valid for narrow strips $l < (\pi/3)a_L$. In this Figure, $a_L u_\epsilon = 30$.

For surfaces with large l (compared to a_L), we can use the same approximation as in equation (18), with $f(u) \approx (a_L u)^{-2}$:

$$\text{Vol}(\bar{A}) = 2\pi^3 R^8 W^2 a_L \int^{u_\epsilon} du u^2 = \pi^3 R^8 \frac{2W^2 a_L}{3\epsilon^3} \quad (25)$$

We see that this area, which is independent of the width, is the same as the area obtained from equation (24) at the extremal value of l , $l = a_L \pi/3$. The situation is illustrated in Figure 2.

To summarize, we obtained the following result for the entanglement entropy density in the dipole theory:

$$\frac{S}{W^2} = \frac{N^2}{2\pi} \frac{2a_L}{3\epsilon^3} G(l/a_L), \quad \text{where } G(z) = \begin{cases} \sin(3z/2) & \text{for } z < \pi/3, \\ 1 & \text{for } z > \pi/3. \end{cases} \quad (26)$$

Entanglement entropy is extensive for very narrow strips, depends on the width of the strip in a nonlinear fashion for widths up to the nonlocality scale and smoothly goes over to a non-extensive (area law) behaviour for wide strips. For wide strips, while the entanglement entropy follows an area law, it has a different form than it would for a generic local theory (given by equation (21)). To explain this, apply reasoning similar to that below equation (21) to a theory with a fixed scale of nonlocality a_L . By definition, the Hamiltonian of such a theory couples together degrees of freedom as far apart at a_L , thus, for a large region, the

dominant part of geometric entanglement entropy should be proportional to the volume of a set of points no more than a_L away from the boundary of A . This volume, for a large enough region, can be approximated by $a_L|\partial A|$, leading to $S \propto a_L|\partial A|/\epsilon^3$, which is exactly what we see in equation (26) for a strip with $l > (\pi/3)a_L$.

Applying our reasoning to the narrow strip, we see that, for $l < a_L$, all degrees of freedom inside the strip should be directly interacting with, and therefore entangled with, degrees of freedom outside of the strip. For a very narrow strip, degrees of freedom inside it will mostly be entangled with the degrees of freedom outside, and entanglement entropy should be proportional to l , which is exactly what we see. As the strip gets wider, some of the degrees of freedom inside the strip become entangled with each other, decreasing the entanglement with the outside and implying a sub-linear growth to the entanglement entropy as a function of l , again in agreement with equation (26).

The exact way in which S deviates from $S \propto l$ can be viewed as a way to probe the distribution of quantum correlations in the ground state of this nonlocal theory. It would be interesting to consider this further.

Finally, notice that above the nonlocality length scale a_L , the shape of the minimal surface is not greatly affected by the exact value of the cutoff; this is a sign that the dipole theory does not have UV/IR mixing. We will see a very different behaviour for the noncommutative theory.

3.3 NCSYM

For entanglement entropy of a strip in the noncommutative theory, the situation is more complicated. As is shown in Figure 3, there are as many as three extremal area surfaces for a given width l of the strip. At large strip widths there is only one surface, for which the relationship between l and u_* approaches that of pure AdS, given by equation (17). At small widths, similarly to the dipole theory, there is a surface which stays close to the cutoff surface.⁸ At intermediate l , there are three extremal surfaces, whose shape is shown in Figure 4. As we will see, the middle of the three surfaces is always unphysical (its area is never smaller than the other two). As the width is increased from zero, at some critical width l_c there is a phase transition as the area of the surface on the top-most branch becomes larger than the area of the surface on the bottom-most branch in Figure 3.

We start by studying top-most branch, which contains surfaces anchored on narrow strips. To study these, we find $u(x)$ as a series expansion for small x . This allows us to write the relationship between l , u_* and u_ϵ for small l :

$$u_\epsilon - u_* = \frac{3}{8} \frac{u_*^3}{1 + (a_\theta u_*)^4} l^2 + \mathcal{O}((l/a_\theta)^4). \quad (27)$$

⁸In [8], this surface was approximated by one placed exactly at the cutoff, at constant u .

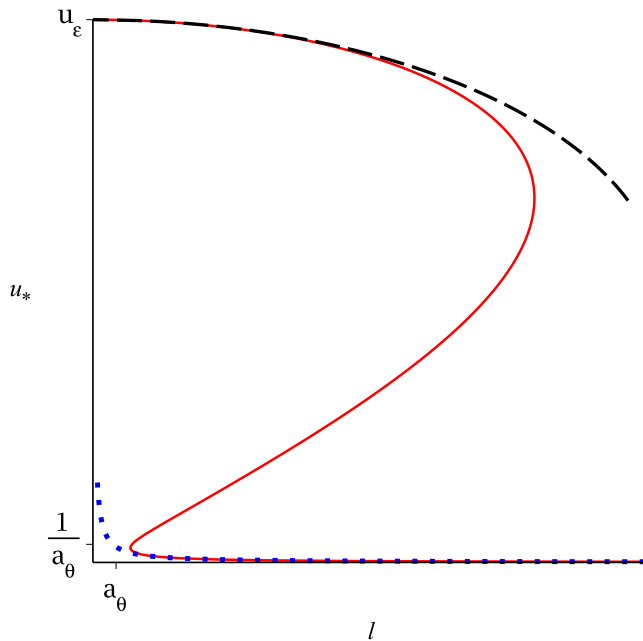


Figure 3: Point of deepest penetration u_* as a function of the strip width l for extremal area surfaces in the gravity dual to the noncommutative theory (solid red line). The blue dotted line shows the result for pure AdS, given by equation (17), while the black dashed line shows the result of equation (27). In this Figure, $a_\theta u_\epsilon = 30$.

The integral in equation (12) can also be expanded and evaluated for small l . Finally, substituting u_* from the expression above into the area integral, we can obtain the area for small l :

$$\text{Vol}(\bar{A}) = \pi^3 R^8 W^2 \left[\frac{l}{\epsilon^3} - \frac{3}{8} \frac{l^3}{a_\theta^4 \epsilon (1 + (\epsilon/a_\theta)^4)} + \mathcal{O}((l/a_\theta)^4) \right]. \quad (28)$$

We have kept the sub-leading terms in ϵ for completeness—expression (28), as given, is correct even for large ϵ as long as l is small.

From equation (27) we see that as we increase u_ϵ keeping l fixed, $(u_\epsilon - u_*) \propto l^2/u_*$, so that $u_\epsilon - u_*$ approaches zero: the minimal surface approaches the boundary surface.

This result turns out to hold even for large (but fixed) strip width l in the large u_ϵ limit. In this limit, we approximate $f(u) \approx (a_\theta u)^4$. This allows us to obtain l and the area as a function of u_* and u_ϵ in terms of hypergeometric functions. We see that l/u_ϵ is a function of the ratio u_*/u_ϵ only. As u_ϵ approaches infinity with l fixed, this ratio goes to 1, showing that the entire minimal surface stays close to the boundary and that our approximation $f(u) \approx (a_\theta u)^4$ is self-consistent even for large l , as long as l is held fixed when the UV cutoff

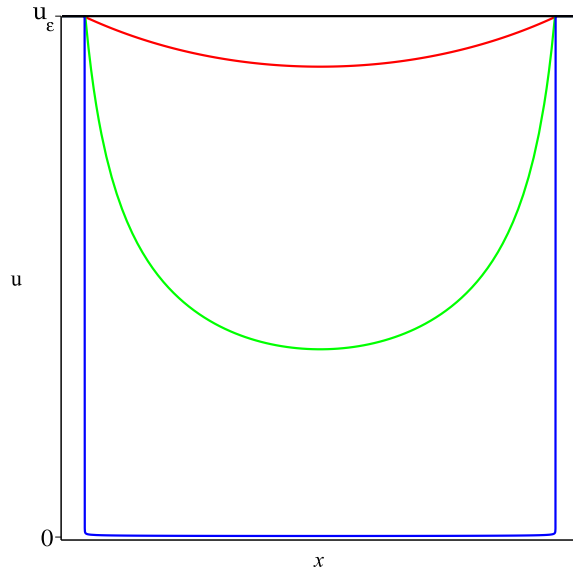


Figure 4: Shape of three extremal area surfaces, given as $u(x)$, all anchored on the same boundary strip.

is removed. The following relationship holds under this approximation:

$$\int_{-l/2}^{l/2} dx \mathcal{L} = \frac{lu_*^3 + u_\epsilon \sqrt{u_\epsilon^6 - u_*^6}}{4}. \quad (29)$$

Thus, the leading order UV divergence of the area of the minimal surface at any fixed width l is

$$\text{Vol}(\bar{A}) = \pi^3 R^8 W^2 \frac{l}{\epsilon^3}. \quad (30)$$

Having understood the top-most branch of the plot in Figure 3, corresponding to surfaces that stay close to the boundary, we now move to the bottom-most one. These surfaces penetrate deeply into the bulk and their shape is not affected by the cutoff point. We can therefore use the same method as before for obtaining their area:

$$\text{Vol}(\bar{A}) = 2\pi^3 R^8 W^2 a_\theta^2 \int^{u_\epsilon} u^3 du = \pi^3 R^8 \frac{W^2 a_\theta^2}{2\epsilon^4}. \quad (31)$$

Since there are multiple extremal surfaces anchored on a strip, we need to find out which of them have the smallest area at a given l . At very small l there is only one surface (see Figure 3), thus, by continuity, for l less than some critical length l_c , the surface of the smallest area corresponds to the top-most branch of Figure 3. Its area is given by equation (30). At l_c there is a first order phase transition.⁹ Above l_c , the surface with the smallest area is on

⁹This is similar to [27] and to [6], as well as to the recent paper [28]. Entanglement entropy is continuous across the transition, but its derivative is not.

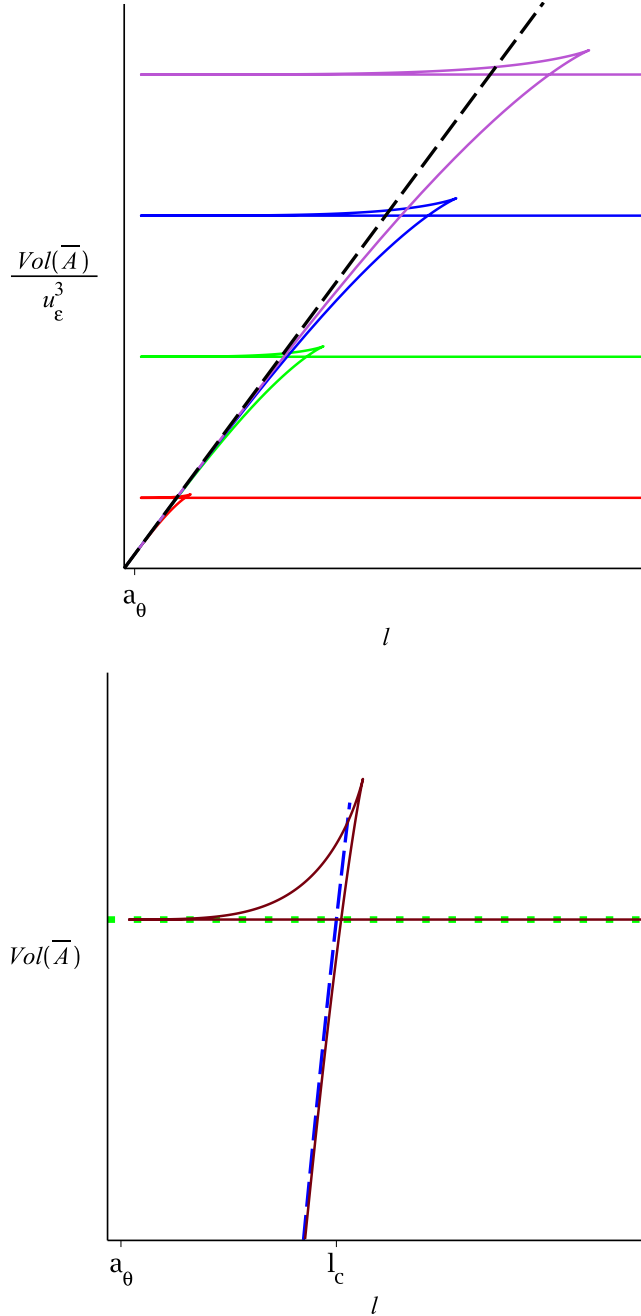


Figure 5: Area of the minimal surface as a function of strip width l for noncommutative theory. Top: Plots with $a_\theta u_\epsilon = 10, 30, 50$ and 70 are shown. Area is scaled by a power of the cutoff to allow functions for different cutoffs to be plotted on the same set of axis. Dashed line corresponds to the leading term in equation (28), $Vol(\bar{A})/u_\epsilon^3 \propto l$. The range of validity of this approximate expression increases with increasing u_ϵ . Bottom: Detail of the fish-tail phase transition is shown. The green dotted line and the blue dashed line correspond to equations (31) and (28) respectively. $a_\theta u_\epsilon = 30$.

the bottom-most branch of Figure 3 and its area is given by equation (31). To compute l_c , we set equations (30) and (31) equal and obtain that $l_c = a_\theta^2 u_\epsilon / 2$.

Since the critical length increases with u_ϵ , if we hold l fixed and take the limit $u_\epsilon \rightarrow \infty$, l_c will diverge to infinity as well and equation (30) will hold for any l .

Our analysis implies that in the limit $\epsilon \rightarrow 0$, the entanglement entropy density for a strip of a fixed length l is

$$\frac{S}{W^2} = \frac{N}{2\pi} \left[\frac{l}{\epsilon^3} - \frac{3}{8} \frac{l^3}{a_\theta^4 \epsilon} + \text{terms vanishing for } \epsilon \rightarrow 0 \right], \quad (32)$$

which, to the leading order, is the same answer as for the dipole theory in the narrow strip limit (equation (26), $l \ll a_L$).

To understand the physics behind this result, we recall that in the noncommutative theory a mode with momentum p_y in the y -direction can be thought of as a dipole field with an effective dipole length θp_y in the x -direction. The high-momentum modes which dominate the divergent part of entanglement entropy all have large effective dipole moments. Therefore the entanglement entropy is that of a nonlocal theory with a large effective scale of nonlocality. This is precisely what we see.

In the complementary limit, fixing a (large) UV cutoff first and then considering wide strips, $l > l_c$, equation (31) shows that entanglement entropy density is equal to

$$\frac{S}{W^2} = \frac{N^2}{2\pi} \frac{a_\theta^2}{2\epsilon^4}. \quad (33)$$

We see that the area law applies and the number of degrees of freedom which are near enough to the boundary of the region to be entangled with the outside is proportional to a_θ^2/ϵ^2 . This is equal to the scale of noncommutativity at the UV cutoff ($a_\theta^2 u_\epsilon = a_\theta^2/\epsilon$) divided by the cutoff length scale ϵ , consistent with our previous discussions.

In the next section, we will compute the entanglement entropy in the noncommutative theory for another geometry: a cylinder whose circular cross-section is in the two noncommutative directions x and y and which is extended infinitely in the commutative direction z . We will obtain a result for the entanglement entropy that is similar to the one in this section, while the geometry of the entangling surfaces will be very different.

4 Entanglement entropy for the cylinder in NCSYM

Consider a region on the boundary extended in the z direction ($-W/2 < z < W/2$, $W \rightarrow \infty$) and satisfying $x^2 + y^2 < l^2$ in the x and y directions. The area functional for a surface homologous to this cylindrical region, assuming rotational symmetry in the $x - y$ plane and translational symmetry in the z direction, is

$$\text{Vol}(\bar{A}) = 2\pi^4 R^8 W \int_0^l dr r (u(r))^3 \sqrt{1 + \frac{(u'(r))^2}{f(u)(u(r))^4}}, \quad (34)$$

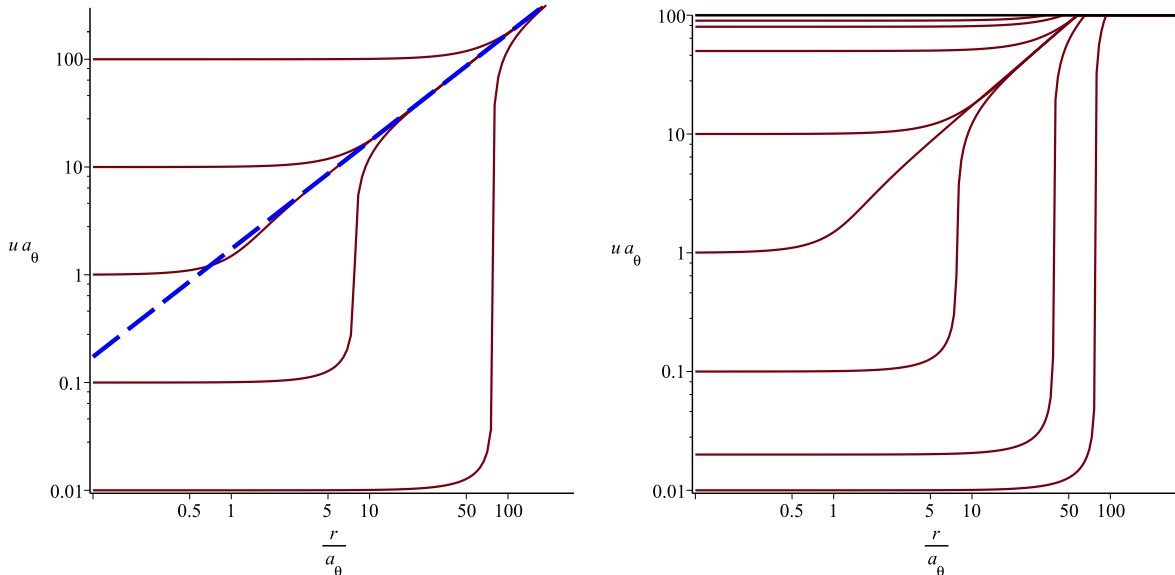


Figure 6: Extremal surfaces homologous to a cylinder in NCSYM, presented as $u(r)$. On the left, the straight dashed line is the asymptotic behaviour given by $a_\theta u = \sqrt{3}r/a_\theta$. On the right, surfaces with l sufficiently smaller or larger than $l_c = a_\theta^2 u_\epsilon / \sqrt{3}$ to reach the cutoff before they had time to approach the this asymptote are shown as well.

where $r = \sqrt{x^2 + y^2}$ and the surface is specified by a function $u(r)$.

Since r appears explicitly in the Lagrangian density, the equation of motion cannot be integrated explicitly even once. We will therefore have to rely more on numerical computation.

Figure 6 shows shapes of extremal surfaces anchored on a disk in the boundary noncommutative theory. As is easy to check analytically, all these surfaces asymptote at large r and u to a single 'cone' given by $a_\theta u = \sqrt{3}r/a_\theta$. A linear analysis about this asymptotic solution gives

$$a_\theta u(r) \approx \sqrt{3}r/a_\theta + t \cos \left(\frac{\sqrt{7}}{2} \ln(r/a_\theta) + \varphi \right), \quad (35)$$

where t and φ are free parameters, with t small. In principle, a relationship between t and φ could be derived given that $u'(0) = 0$, but it cannot be obtained within perturbation theory. It is interesting and perhaps surprising that the fluctuations about the asymptote are oscillatory in r . This behaviour, which can be seen in Figure 6, agrees very well with more detailed numerical analysis.

From Figure 6 we see that surfaces with u_* relatively close to a_θ^{-1} approach the asymptote $u = \sqrt{3}r/a_\theta^2$ before reaching the cutoff, while those with large u_* ($a_\theta u_* \gg 1$) or small u_* ($a_\theta u_* \ll 1$) do not. At a fixed cutoff, then, we have three classes of surfaces: shallowly

probing surfaces, $a_\theta u_* \gg 1$, with l smaller than and bounded away from $l_c := a_\theta^2 u_\epsilon / \sqrt{3}$, deeply probing surfaces, $a_\theta u_* \ll 1$, with l larger than and bounded away from l_c and the intermediate category, for which l is approximately equal to l_c . In the first and second category, there is a unique extremal surface at a given radius l , while for radii close to l_c the situation is more complicated, due to the oscillatory nature of the near-asymptotic solutions shown in equation (35). Since the cutoff radius l_c increases with u_ϵ (similar to the behaviour in the strip geometry), the entanglement surface for a region with any radius l belongs to the first category for a sufficiently high UV cutoff.

First, let us consider the surfaces with small l/a_θ . These can be studied by expanding in l/a_θ . We get the following two results:

$$u_\epsilon - u_* = \frac{3}{4} \frac{u_*^3}{1 + (a_\theta u_*)^4} l^2 + \mathcal{O}((l/a_\theta)^4), \quad (36)$$

$$\text{Vol}(\bar{A}) = 2\pi^4 R^8 W \left[\frac{l^2}{2\epsilon^3} - \frac{9}{32} \frac{l^4}{a_\theta^4 \epsilon (1 + (\epsilon/a_\theta)^4)} + \mathcal{O}((l/a_\theta)^4) \right]. \quad (37)$$

The l/a_θ expansion for the area of the minimal surface has a structure which is similar to the one we obtained for the strip in the noncommutative theory: organizing the expansion in powers of l , the term of order l^n has as its leading ϵ dependence $1/\epsilon^{5-n}$ (with n even). Assuming that this analytic structure is valid for finite l/a_θ , we obtain that in the limit $\epsilon \rightarrow 0$, the entanglement entropy density for a cylinder at a fixed radius l is

$$\frac{S}{W} = \frac{N}{2\pi} \left[\frac{\pi l^2}{\epsilon^3} - \frac{9}{32} \frac{l^4}{a_\theta^4 \epsilon} + \text{terms vanishing for } \epsilon \rightarrow 0 \right]. \quad (38)$$

Qualitatively, this is the same answer as we obtained for the strip: entanglement entropy is extensive, proportional to the volume of the considered region. Notice that neither expression has a non-zero universal (independent of ϵ part).

At finite (and large) cutoff, we can consider large radius cylinders. For l sufficiently larger than l_c we see from Figure 6 that $u_* a_\theta \ll 1$ and the entangling surface seems close in shape to that in pure AdS (as it approaches the boundary at approximately the right angle, based on numerical evidence). Thus, $u_* \propto l^{-1}$ and the area is approximately

$$\text{Vol}(\bar{A}) = 2\pi^4 R^8 W a_\theta^2 \int dr r u^3 u'(r) = 2\pi^4 R^8 W a_\theta^2 l \int^{u_\epsilon} du u^3 = \pi^3 R^8 \frac{2\pi l W a_\theta^2}{4\epsilon^4}, \quad (39)$$

where we have used $f(u) \approx (a_\theta u)^{-4}$ and approximated $r \approx l$ in the region near the boundary. Resulting entanglement entropy has the same interpretation as the one in equation (33), with the area of the strip's boundary, W^2 replaced by the area of the boundary of the cylinder, $2\pi l W$.

Having understood the minimal surface in the large l and small l limits, we now turn to l near the cutoff radius $l_c = a_\theta^2 u_\epsilon / \sqrt{3}$, which corresponds to $u_* a_\theta$ close to 1. Figure 7 shows

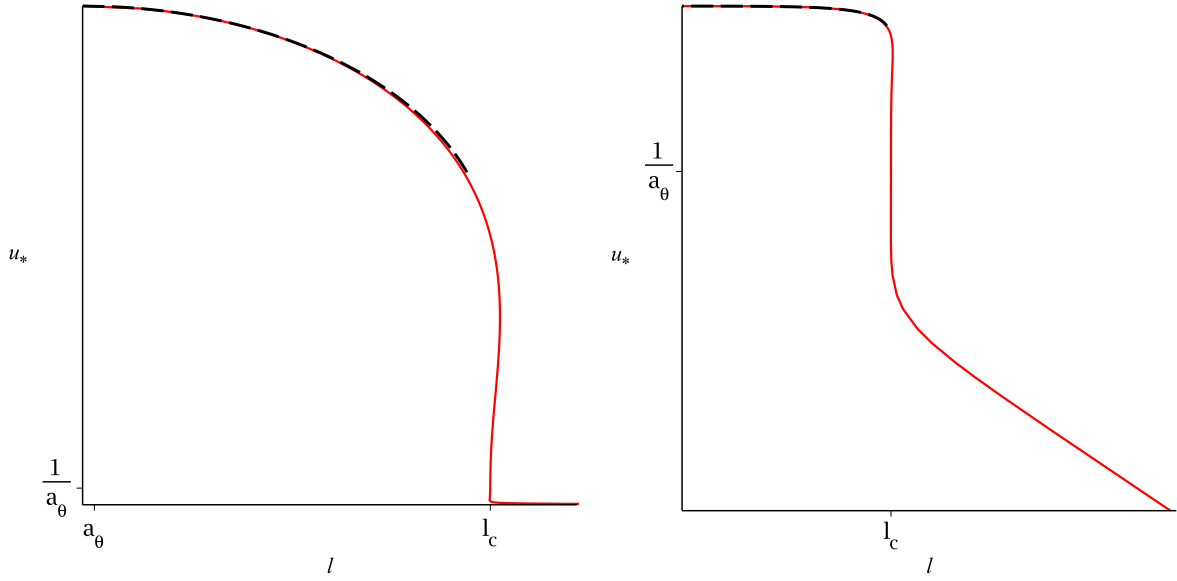


Figure 7: Point of deepest penetration u_* as a function of the cylinder's radius l for the minimal surface homologous to a cylinder in the noncommutative theory. The black dashed line corresponds to equation (36). Linear scale on the left, log-log scale on the right; $a_\theta u_\epsilon = 30$ for both plots.

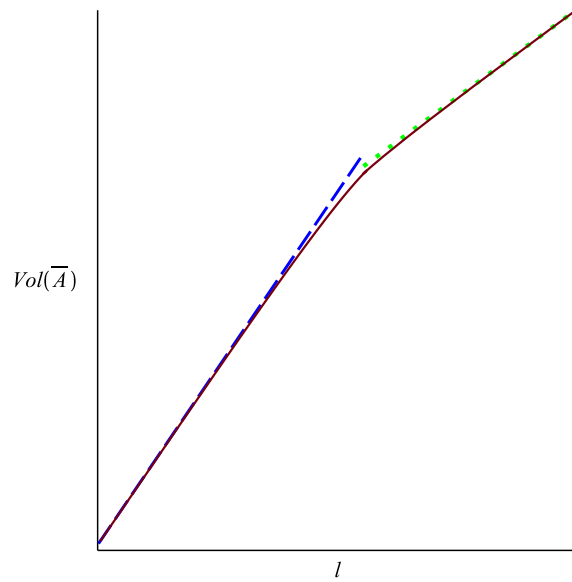


Figure 8: Area of the minimal surface homologous to a cylinder, as a function of the cylinder's radius l , with both axis shown in logarithmic scale. $a_\theta u_\epsilon = 30$. The green dotted line and the blue dashed line correspond to equations (39) and (37) respectively.

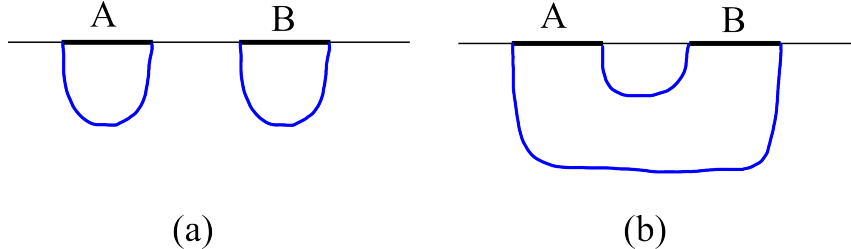


Figure 9: Minimal surface for a union of two disjoint regions $A \cup B$ can have one of two topologies: (a) disconnected or (b) connected.

the dependence of u_* on l over the entire range for a finite cutoff. We notice that near l_c , there are multiple values of u_* at a given l : just like in the case of the strip, there is a range of radii l for which there exist multiple extremal surfaces anchored on the same cylinder. This is related to the oscillating nature of the asymptotic solution (35). Since taking a large cutoff limit removes the radius l_c , at which phase transition takes place, to infinity, we will not attempt a detailed study of the properties of the phase transition, which is complicated by the oscillatory nature of the minimal surfaces near the critical radius.

It is interesting to notice that, apart from the details of the phase transition, the entanglement entropy for the cylinder has the same qualitative behaviour as it does for the strip, even though the geometry of the minimal surfaces is very different.

5 Mutual information in NCSYM

To strengthen our discussion of UV/IR mixing in noncommutative SYM theory, it would be interesting to study the behaviour of an observable that (in the commutative theory) is finite in the large UV cutoff limit. One such observable is mutual information.

Consider two disjoint regions A and B . Mutual information is defined by $I(A, B) := S(A) + S(B) - S(A \cup B)$. Subadditivity implies that mutual information is a non-negative quantity. For local theories, holographic mutual information is UV finite, since contributions from the near-boundary parts of the minimal surfaces cancel. It is known to exhibit a phase transition [29]: if the regions A and B have width l and the distance between them is x , $I(A, B)$ is nonzero for x less than some x_c and zero for x greater than x_c , with x_c/l of order 1. The origin of this phase transition is shown in Figure 9: for large x/l , the minimal area surface has the topology shown in 9(a), while for small x/l , it has the topology shown in 9(b). Behaviour of mutual information and the existence or disappearance of this phase transition can be used to find characteristic length scales, see for example [30] and [31]. For NCSYM we find that the mutual information phase transition is absent for length scales less than l_c . The fact that l_c depends on the UV cutoff is then a signature of the UV/IR mixing.

To study the details of this signature, let regions A and B be strips of width l_A and l_B respectively, separated by a distance x . Then, if l_A , l_B and x are held fixed as the cutoff u_ϵ is taken to infinity, entanglement entropies associated with strips of width x , l_A , l_B and $l_A + l_B + x$ are all extensive. Therefore, $S(l_A) + S(l_B) < S(l_A + l_B + x) + S(x)$, i.e. the surface in Figure 9(a) has a smaller area than that in Figure 9(b). This implies that $I(A, B) = 0$ for any x and there is no phase transition. On the other hand, if l_A and l_B are both larger than l_c , then $S(l_A) \approx S(l_B) \approx S(l_A + l_B + x)$ because to leading order the entanglement entropies do not depend on the width of the strip. Mutual information is positive (and divergent, since entanglement entropy in the noncommutative theory does not have a UV-finite piece) as long as x is small enough and undergoes a phase transition as x is increased just like it does for a local field theory.

It would be interesting to study the behaviour of mutual information near the phase transition in detail. We leave this to future work.

6 Final comments

A key ingredient in our analysis was keeping the cutoff finite, if large. Only when the entangling region A is placed on a cutoff surface at finite $u = u_\epsilon$ can the correct minimal area minimal surfaces be found. This is especially true in the noncommutative theory, where UV/IR mixing implies that infrared physics is affected by the precise value of the cutoff.

We have already discussed the origins of the dependence of the entanglement entropy on the size (volume or area) of the region A , on the cutoff length ϵ and on the intrinsic length scales a_L and a_θ built into our nonlocal theories. The numerical coefficients we obtain are of physical significance: In the volume law regime, the coefficient measures whether degrees of freedom inside of A are entangled with the outside of A or with each other. Therefore, this coefficient controls the maximum size of the region over which the theory thermalizes [9]. A similar statement can be made about the coefficient in the area law regime.

While the open string metric gives distances in the nonlocal boundary field theory, it is the closed string metric that determines the causal structure of the theory. In a local field theory, knowledge of the density matrix ρ_A in the region A is enough to compute all observables within the domain of dependence of A . While we don't know exactly which portion of the total holographic dual spacetime is dual to ρ_A itself [32, 33, 34, 35], the answer must involve the bulk (closed string) metric and its causal structure. Applying this argument to our nonlocal theories, we see that it is the bulk metric that determines the extent of the holographic dual to the density matrix ρ_A . For example, this holographic dual might be bounded by the minimal surface. Then, the intersection between the AdS boundary and the lightsheets originating from the minimal surface might be interpreted as the boundary of the “domain of dependence” of the region A in a nonlocal theory. We would expect that

knowledge of the density matrix ρ_A would be sufficient to determine all observables within this “domain of dependence”. This new “domain of dependence” is determined causally not by the open string metric but by the bulk closed string metric at a fixed cutoff. This closed string metric is not isotropic, in fact, it has a very large “speed of light” in the nonlocal directions, compared with the open string metric. Field theory computations show that nonlocal field theories have large propagation speeds, see for example the behaviour discussed in [18], or the observations that the propagation speed in the noncommutative theory is effectively infinite [36, 37]. As a result, in a nonlocal theory the “domain of dependence” should have a very small time-like extent. This is consistent with it being bound by lightsheets which originate on a minimal surface which does penetrate the bulk very far, a feature we have observed.

A related feature of our minimal surfaces is that they are not necessarily orthogonal to the boundary at a finite cutoff. Therefore, for example, the two proposals given in [38] for a covariant version of holographic entanglement entropy are not necessarily equivalent, raising an interesting question about time-dependent nonlocal theories. Similarly, arguments for strong subadditivity of covariant holographic entanglement entropy in time dependent spacetimes, in [39], do not apply either (however, the simple argument for static spacetimes, in [40], does apply, and therefore the entanglement entropies computed in this paper do satisfy strong subadditivity).

Since our computations were done using holography, they are reliable in the strong coupling limit. It would be interesting to see whether the same results apply at weak coupling, with the appropriate nonlocal scale, a_θ or a_L , replaced by its weak coupling counterpart, $\sqrt{\theta}$ or L respectively. This might not necessarily be the case: for example, the enhancement to the rate of dissipation provided by noncommutativity at strong coupling is not seen at weak coupling [13]. The analysis in [13] points towards strong coupling being necessary for scrambling in noncommutative theory, and, if the results in [9] can be extended to this situation, strong coupling being necessary for extensive entanglement entropy. It would be interesting to settle this question by a direct computation of geometric entanglement entropy in a weakly coupled noncommutative theory. Unfortunately, it will not be possible to learn anything from free noncommutative theories as these are equivalent to their commutative counterparts.

A simple example of a nonlocal field theory with volume scaling of its entanglement entropy was given in [41]. In that work, it was proposed that volume scaling was a necessary feature of entanglement entropy in a hypothetical field theory dual to flat space. In contrast to this hypothetical theory, our nonlocal theories do not have vanishing correlation functions.

Finally, it would be interesting to study other extremal surfaces in holographic duals to nonlocal theories, following the work for local theories [42], as well as to extend our results to finite temperature.

Acknowledgments

We are grateful for helpful discussions with Keshav Dasgupta, Ori Ganor, Nima Lashkari, Shunji Matsuura and Mark van Raamsdonk. This work was completed with support from the Natural Sciences and Engineering Council of Canada (NSERC).

References

- [1] S. Ryu and T. Takayanagi, *Holographic derivation of entanglement entropy from AdS/CFT*, *Phys.Rev.Lett.* **96** (2006) 181602, [[hep-th/0603001](#)].
- [2] T. Nishioka, S. Ryu, and T. Takayanagi, *Holographic Entanglement Entropy: An Overview*, *J.Phys.* **A42** (2009) 504008, [[arXiv:0905.0932](#)].
- [3] T. Takayanagi, *Entanglement Entropy from a Holographic Viewpoint*, *Class.Quant.Grav.* **29** (2012) 153001, [[arXiv:1204.2450](#)].
- [4] S. Ryu and T. Takayanagi, *Aspects of Holographic Entanglement Entropy*, *JHEP* **0608** (2006) 045, [[hep-th/0605073](#)].
- [5] T. Nishioka and T. Takayanagi, *AdS Bubbles, Entropy and Closed String Tachyons*, *JHEP* **0701** (2007) 090, [[hep-th/0611035](#)].
- [6] I. R. Klebanov, D. Kutasov, and A. Murugan, *Entanglement as a probe of confinement*, *Nucl.Phys.* **B796** (2008) 274–293, [[arXiv:0709.2140](#)].
- [7] J. Eisert, M. Cramer, and M. Plenio, *Area laws for the entanglement entropy - a review*, *Rev.Mod.Phys.* **82** (2010) 277–306, [[arXiv:0808.3773](#)].
- [8] J. L. Barbon and C. A. Fuertes, *Holographic entanglement entropy probes (non)locality*, *JHEP* **0804** (2008) 096, [[arXiv:0803.1928](#)].
- [9] N. Lashkari, *Equilibration of Small and Large Subsystems in Field Theories and Matrix Models*, [arXiv:1304.6416](#).
- [10] Y. Sekino and L. Susskind, *Fast Scramblers*, *JHEP* **0810** (2008) 065, [[arXiv:0808.2096](#)].
- [11] M. Requardt, *Entanglement-Entropy for Groundstates, Low-lying and Highly Excited Eigenstates of General (Lattice) Hamiltonians*, [hep-th/0605142](#).
- [12] V. Alba, M. Fagotti, and P. Calabrese, *Entanglement entropy of excited states*, *Journal of Statistical Mechanics: Theory and Experiment* **2009** (2009), no. 10 P10020.

- [13] M. Edalati, W. Fischler, J. F. Pedraza, and W. Tangarife Garcia, *Fast Scramblers and Non-commutative Gauge Theories*, *JHEP* **1207** (2012) 043, [[arXiv:1204.5748](#)].
- [14] J. L. Barbon and C. A. Fuertes, *A Note on the extensivity of the holographic entanglement entropy*, *JHEP* **0805** (2008) 053, [[arXiv:0801.2153](#)].
- [15] W. Fischler, A. Kundu, and S. Kundu, *Holographic Entanglement in a Noncommutative Gauge Theory*, [arXiv:1307.2932](#).
- [16] A. Hashimoto and N. Itzhaki, *Noncommutative Yang-Mills and the AdS / CFT correspondence*, *Phys.Lett.* **B465** (1999) 142–147, [[hep-th/9907166](#)].
- [17] J. M. Maldacena and J. G. Russo, *Large N limit of noncommutative gauge theories*, *JHEP* **9909** (1999) 025, [[hep-th/9908134](#)].
- [18] S. Minwalla, M. Van Raamsdonk, and N. Seiberg, *Noncommutative perturbative dynamics*, *JHEP* **0002** (2000) 020, [[hep-th/9912072](#)].
- [19] N. Seiberg and E. Witten, *String theory and noncommutative geometry*, *JHEP* **9909** (1999) 032, [[hep-th/9908142](#)].
- [20] M. Li and Y.-S. Wu, *Holography and noncommutative Yang-Mills*, *Phys.Rev.Lett.* **84** (2000) 2084–2087, [[hep-th/9909085](#)].
- [21] S. Chakravarty, K. Dasgupta, O. J. Ganor, and G. Rajesh, *Pinned branes and new nonLorentz invariant theories*, *Nucl.Phys.* **B587** (2000) 228–248, [[hep-th/0002175](#)].
- [22] A. Bergman and O. J. Ganor, *Dipoles, twists and noncommutative gauge theory*, *JHEP* **0010** (2000) 018, [[hep-th/0008030](#)].
- [23] K. Dasgupta, O. J. Ganor, and G. Rajesh, *Vector deformations of N=4 superYang-Mills theory, pinned branes, and arched strings*, *JHEP* **0104** (2001) 034, [[hep-th/0010072](#)].
- [24] A. Bergman, K. Dasgupta, O. J. Ganor, J. L. Karczmarek, and G. Rajesh, *Nonlocal field theories and their gravity duals*, *Phys.Rev.* **D65** (2002) 066005, [[hep-th/0103090](#)].
- [25] E. Bergshoeff, C. M. Hull, and T. Ortin, *Duality in the type II superstring effective action*, *Nucl.Phys.* **B451** (1995) 547–578, [[hep-th/9504081](#)].
- [26] K. Dasgupta and M. Sheikh-Jabbari, *Noncommutative dipole field theories*, *JHEP* **0202** (2002) 002, [[hep-th/0112064](#)].
- [27] K. Narayan, T. Takayanagi, and S. P. Trivedi, *AdS plane waves and entanglement entropy*, *JHEP* **1304** (2013) 051, [[arXiv:1212.4328](#)].

- [28] V. E. Hubeny, H. Maxfield, M. Rangamani, and E. Tonni, *Holographic entanglement plateaux*, [arXiv:1306.4004](#).
- [29] M. Headrick, *Entanglement Renyi entropies in holographic theories*, *Phys.Rev.* **D82** (2010) 126010, [[arXiv:1006.0047](#)].
- [30] E. Tonni, *Holographic entanglement entropy: near horizon geometry and disconnected regions*, *JHEP* **1105** (2011) 004, [[arXiv:1011.0166](#)].
- [31] W. Fischler, A. Kundu, and S. Kundu, *Holographic Mutual Information at Finite Temperature*, [arXiv:1212.4764](#).
- [32] R. Bousso, S. Leichenauer, and V. Rosenhaus, *Light-sheets and AdS/CFT*, *Phys.Rev.* **D86** (2012) 046009, [[arXiv:1203.6619](#)].
- [33] B. Czech, J. L. Karczmarek, F. Nogueira, and M. Van Raamsdonk, *The Gravity Dual of a Density Matrix*, *Class.Quant.Grav.* **29** (2012) 155009, [[arXiv:1204.1330](#)].
- [34] V. E. Hubeny and M. Rangamani, *Causal Holographic Information*, *JHEP* **1206** (2012) 114, [[arXiv:1204.1698](#)].
- [35] R. Bousso, B. Freivogel, S. Leichenauer, V. Rosenhaus, and C. Zukowski, *Null Geodesics, Local CFT Operators and AdS/CFT for Subregions*, [arXiv:1209.4641](#).
- [36] A. Hashimoto and N. Itzhaki, *Traveling faster than the speed of light in noncommutative geometry*, *Phys.Rev.* **D63** (2001) 126004, [[hep-th/0012093](#)].
- [37] B. Durhuus and T. Jonsson, *Noncommutative waves have infinite propagation speed*, *JHEP* **0410** (2004) 050, [[hep-th/0408190](#)].
- [38] V. E. Hubeny, M. Rangamani, and T. Takayanagi, *A Covariant holographic entanglement entropy proposal*, *JHEP* **0707** (2007) 062, [[arXiv:0705.0016](#)].
- [39] A. C. Wall, *Maximin Surfaces, and the Strong Subadditivity of the Covariant Holographic Entanglement Entropy*, [arXiv:1211.3494](#).
- [40] M. Headrick and T. Takayanagi, *A Holographic proof of the strong subadditivity of entanglement entropy*, *Phys.Rev.* **D76** (2007) 106013, [[arXiv:0704.3719](#)].
- [41] W. Li and T. Takayanagi, *Holography and Entanglement in Flat Spacetime*, *Phys.Rev.Lett.* **106** (2011) 141301, [[arXiv:1010.3700](#)].
- [42] V. E. Hubeny, *Extremal surfaces as bulk probes in AdS/CFT*, *JHEP* **1207** (2012) 093, [[arXiv:1203.1044](#)].